

Direct Assessment of Profilometric Roughness Variability from Typical Implant Surface Types

Sean S. Kohles, PhD¹/Melissa B. Clark, MS²/Christopher A. Brown, PhD³/James N. Kenealy, PharmD⁴

Purpose: Protocols for quantifying the surface roughness of implants are varied and dependent upon the roughness parameter produced by the particular measurement device. The objective of this study was to examine the accuracy and precision of typical roughness characterization instruments used in the dental implant industry. **Materials and Methods:** The average roughness (Ra) was measured using 2 common surface characterization instruments: an interferometer and a stylus profilometer. Titanium disks were prepared to represent 4 typical dental implant surfaces: machined, acid-etched, hydroxyapatite-coated, and titanium plasma-sprayed. Repeated measurements from multiple sites on each surface were undertaken to establish statistical inferences. Qualitative images of the surfaces were also acquired using a laser scanning confocal microscope. After surface measurements were conducted, the disks were diametrically cut and cross-sectional profiles were examined using a scanning electron microscope (SEM) as a comparative measure of surface topography. An analysis of variance was applied to isolate the effects of the measurement site, measurement sequence, surface treatment, and instrument type on Ra values. **Results:** The results indicated that surface treatment ($P = .0001$) and instrument ($P = .0001$) strongly influenced Ra data. By design, measurement site (diametrical: $P = .9859$; area: $P = .9824$) and measurement sequence ($P = .9990$) did not influence roughness. In the assessment of individual instrument accuracy, the interferometer was the most accurate in predicting SEM-based roughness ($P = .6688$) compared with the stylus ($P = .0839$). As a measure of aggregate precision over all measurements, the most repeatable instrument was the stylus (coefficient of variation [CV] = 0.108), followed by the interferometer (CV = 0.125) and SEM (CV = 0.273). **Discussion:** These results indicate dependencies in accuracy and precision related to the surface characterization technique. **Conclusion:** Instrument variability may obscure functional correlations between implant surface topography and osseointegration. *INT J ORAL MAXILLOFACIAL IMPLANTS* 2004;19:510–516

Key words: implant surfaces, profilometry, surface metrology

¹Director, Kohles Bioengineering, Portland, Oregon; Adjunct Associate Professor, Department of Mechanical Engineering, Portland State University, Portland, Oregon; Adjunct Associate Professor, Department of Surgery, Oregon Health & Science University, Portland, Oregon.

²Patient Coordinator, Rhode Island Orthodontic Group, East Greenwich, Rhode Island.

³Saint-Gobain Professor and Director, Surface Metrology Laboratory, Department of Mechanical Engineering, Worcester Polytechnic Institute, Worcester, Massachusetts.

⁴Director, Clinical Research, Implant Innovations, Palm Beach Gardens, Florida.

Correspondence to: Dr Sean S. Kohles, Kohles Bioengineering, 1731 SE 37th Avenue, Portland, OR 97214-5135. Fax: +503 231 5504. E-mail: ssk@kohlesbioengineering.com.

Presented in part at the 26th Annual Institute of Electrical and Electronics Engineers Northeast Bioengineering Conference, April 8–9, 2000, Storrs, Connecticut, and the Fall Annual Meeting of the Biomedical Engineering Society, October 12–14, 2000, Seattle, Washington.

To replace teeth in a partially or completely edentulous patient, the use of dental implants has become a viable alternative to fixed partial denture restorations. Endosseous implants gain initial stability from a precise fit with the supporting bone. Studies using commercially pure titanium implants in animal models have shown that implant anchorage can be achieved with direct bone contact and enhanced by increasing the surface roughness of the implant.^{1–9}

The percentage of bone-implant contact has been shown to relate to successful implant function.¹⁰ Animal studies have demonstrated that regions with cancellous bone, such as the posterior maxilla, offer statistically lower success rates when compared with locations with denser tissue.¹¹ This is related to the fact that denser bone increases the amount of bone-implant surface contact. Although the anatomic surface availability cannot be controlled, the surface

topography of an implant can be designed to increase bone-implant contact. Attempts have been made to improve implant anchorage by increasing the bone-implant surface contact through porous or coated implant surfaces. Studies that have examined the biologic development of the bone-implant interface resulting from a variety of implant surface treatments indicate that long-term fixation, assessed by mechanics and histomorphometry, can be attained by increasing roughness of the implant surface, thereby increasing bone-implant contact.^{6,8,11,12}

A number of implant surface treatments exist that roughen surface topography and thus offer a means to improve fixation. Rough surfaces are produced through the addition or subtraction of implant surface material. A plasma arc spraying process can be used to add a coating such as hydroxyapatite (HA) or bioactive calcium phosphate (CaP).¹³ The coating material is generally fed into a plasma flame in powder form by a carrier gas, where it melts, gains high velocity because of high plasma enthalpies, and is propelled to the substrate surface.^{14,15} Alternatively, treatments such as polishing, machining, and acid etching subtract material from the implant surface. In polishing, an abrasive material is attached to a flexible backing, such as a wheel or a belt. The substrate is then brought into direct contact with the abrasive surface. Usually polishing is started with a coarse abrasive paper (50 to 220 grit) followed by a finer abrasive (generally about 600 grit) at a polishing speed of 10 to 30 m/s. The process of acid etching produces a matte finish on metallic substrates. This process removes oxide films and embedded surface contaminants while roughening the surface. Hydrochloric, nitric, phosphoric, chromic, or sulfuric acids are generally combined with salts to achieve a rougher substrate surface.¹⁴ Finally, blasting both adds and subtracts surface material. Abrasive aluminum oxide (Al_2O_3) or titanium dioxide (TiO_2) particles 0.12 to 0.25 mm in diameter are impinged upon the surface of the implant. The implant is roughened both by the barrage and by embedded particles.^{14,16}

A variety of devices exist for characterizing the resulting roughness of the applied surface treatments. These can be divided into 3 categories of instruments: mechanical contact profilometers, scanning probe microscopes, and optical profilometers. Stylus-based profilometers are common. These devices convert the vertical motion of a phonograph-like stylus (often diamond-tipped, with a radius of 2 to 20 μm) as it moves across the surface into electrical signals that are plotted against distance traversed.

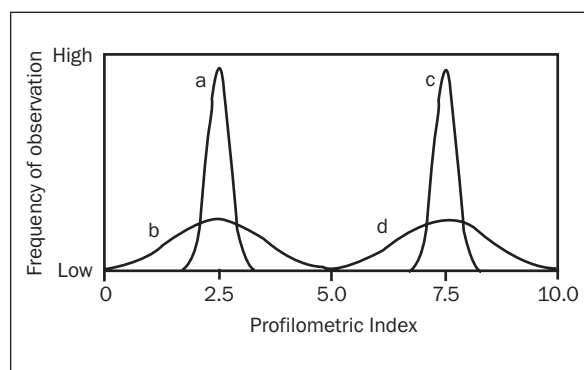


Fig 1 Hypothetical comparison of 4 normally distributed profilometric measurements. If a roughness index of 2.5 is determined to be the actual measure of surface quality, the 4 sets of profilometric measurements can be categorized as (a) accurate and precise, (b) accurate but imprecise, (c) precise but inaccurate, (d) imprecise and inaccurate.

An atomic force microscope is an example of a scanning probe microscope. It utilizes a stylus mounted to the end of a cantilever. Atomic forces attract the fine-tipped stylus (6 to 60 nm radius) to the surface, and the reaction force generated during cantilever bending is used to indicate the surface profile.¹⁷ Laser confocal profilometers and interferometers do not mechanically contact the surface; they utilize a light beam as an optical stylus to obtain a surface profile.¹⁸ The beam width, aperture, and wave length determine the lateral resolution. Each of these techniques provides a means to quantify and qualify rough surfaces for biomedical applications.

The potential for variation exists in the measurement of surface roughness resulting from the available surface preparation techniques. Surface metrology indicates that a variety of assumptions and surface parameters influence a spectrum of roughness metrics.^{12,19-22} Since implant surface quality has been shown to affect long-term stability, industry-wide standardization of acceptable levels of accuracy and precision for each measurement device is necessary to ensure consistent characterization of commercially available implants. However, protocols for quantifying the resulting roughness are still varied and dependent upon the specific parameter produced by the particular measurement device.²³

The objective of this project was to characterize the accuracy and precision of representative dental implant profilometry techniques (Fig 1). To satisfy this objective, 2 common profilometers were used to quantify 4 different surfaces for comparison with cross-sectional views analyzed with microscopy.

MATERIALS AND METHODS

Repeated measurements of multiple controlled surface preparations were made using 2 common instruments: a stylus profilometer and an interferometer. Commercially pure titanium disks were prepared to represent typical implant surface types: machined (untreated), acid-etched, titanium plasma-sprayed (TPS), and HA-coated. The disk shape was designed to eliminate roughness or measurement dependencies upon geometry or sampling location. Seventy-two disks (5 mm diameter \times 1 mm thick) were prepared by Implant Innovations, Palm Beach Gardens, Florida. Four disks, each with 1 of the 4 surface conditions, were randomly selected for repeated-measures analysis. The transverse cross sections were examined using microscopy to establish an actual value of surface quality to evaluate accuracy. The accuracy of each measurement technique was quantified by comparing instrument-derived values and values derived by measuring cross-sectional profiles of each surface type created using a scanning electron microscope (SEM; JSM-840; JEOL USA, Peabody, MA) at 400 \times magnification. A laser scanning confocal microscope (LSCM; Biorad MRC 1024ES; JEOL USA) with a krypton-argon laser also provided qualitative information about the surface topographies.

A power analysis was applied to initial data sets to ensure the statistical strength of the final sample sizes. Using preliminary standard deviation data (σ_i) from 5 samples per surface condition (i), it was assumed that the probability of the measurements would be within 95% of the sample means ($Z_{\alpha/2} = 1.96$) with a margin of error (B) of = 10%. Thus the normal, standard error of the estimator equation, comparing 2 surfaces, resulted in a sample size of

$$n = \left[\frac{Z_{\alpha}}{2} \right]^2 \cdot \frac{[\sigma_1^2 + \sigma_2^2]}{B^2}$$

for equal sized groups. This power study indicated that 15 measurements should be collected from each individual site on each of the 4 surface types.

Multiple measurements were taken of each surface with each profilometer from sample disks. Linear measurements (2-dimensional data) were taken along 2 perpendicular diameters using a stylus profilometer (Mahr Perthometer PRK; Mahr Federal, Cincinnati, OH). A 5- μ m-radius stylus tip was used for all 120 measurements (2 diameters \times 15 measurements \times 4 surface types). Filtered and unfiltered data were acquired as the stylus moved across the surface at 0.50 mm/s. Areal measurements (3-dimensional data) within the 4 quadrants defined by the

stylus bisections were then taken using an interferometer (NewView 5000; Zygo, Middlefield, CT). Light and dark fringe patterns were processed from the optical path difference between a reference white-light beam and 1 reflected from sample surfaces. The measurements were taken with a 20 \times objective lens and a 20 \times instrument magnification, for a total magnification of 400 \times , over each 378 \times 268- μ m quadrant. The camera resolution was 1.2 μ m, and a low-pass median filter was used for all 240 measurements (4 quadrants \times 15 measurements \times 4 surface types). The filter provided a means to optimize the fringe pattern without affecting resolution. Qualitative information about the surface, ie, images, was collected using the LSCM at a 20 \times magnification objective and a 16 \times instrument magnification for a total magnification of 320 \times over each 844.6 \times 844.6- μ m region. All 2- and 3-dimensional quantitative roughness calculations were determined using software developed for scale sensitive-fractal analysis (Surfrax; Surftract, Norwich, VT). The validated software provided consistent analysis between profilometers. It used a patchwork method to determine area-scale fractal properties of measured surfaces.²⁴

Single representative disk samples of each surface were then diametrically cut through their geometric centers (Isomet 11-1180 Low Speed Saw; Buehler, Lake Bluff, IL, and 220 Grit Diamond Grinding Wheel; Norton, Worcester, MA). The exposed cross section was polished to clarify the edge of the analyzed roughened surface, following published histomorphometric techniques.²⁵ Four length segment images along the cut edge of each roughened surface were viewed from an orientation orthogonal to the exposed cross-section under the SEM, and a digital trace of the surface profile was produced. A magnification of 400 \times was used, which gave a sampling length of 219 μ m. The profile was analyzed using image analysis software (Scion Image; Scion, Frederick, MD) where maximum and minimum lines were drawn at the highest peak and lowest valley. The mean line was determined by equating the areas defined by the profile curve above and below the minimum and maximum lines, respectively (Fig 2). The distance from the mean line to the contours of this profile edge (z) as a function of incremental length (x) was used to directly calculate a center-line average roughness value (Ra) using the following equation:

$$Ra = \frac{1}{L} \int_0^L |z(x)| dx$$

along the measurement length (L). This roughness metric was used as the basis for an accuracy comparison among the instruments.

Descriptive and comparative statistical analyses tested the effects of specific measurement site, measurement sequence, measurement precision, surface treatment, and instrument type on all Ra values. An analysis of variance was applied to determine the statistical significance of any influence by calculating how much of the variability in the dependent variable (roughness) could be explained by each of the effects in question. The resulting probability (P) was a guide to how important that effect was in explaining the behavior of the dependent variable. Where $P < .05$, the independent variable was considered to have influenced the behavior of the dependent variable. Fisher's protected least significant difference (PLSD) test was applied post hoc for direct effect comparisons. Although the effect of repeatability (measurement site and sequence as nominal independent variables) was statistically analyzed using analysis of variance, the degree of instrument precision was quantified using both site-specific and aggregate coefficients of variation ($CV = \text{standard deviation/mean}$) for all measurements made by each instrument. Statistical analyses were performed using commercially available software (StatView v5.0.1, SAS Institute, Cary, NC). Roughness values are reported as means and standard errors (SEs).

RESULTS

Qualitative images from an LSCM indicate the unique visual characteristics of each implant surface type (Fig 3). Note the more granular appearance of HA-coated and TPS surfaces. Cross sections, as examined using an SEM (Fig 4), provided a means to directly quantify surface topography from digitized profiles of each implant surface type. This perspective helped to identify local characteristics that may have influenced the profilometry-derived Ra values.

Overall results indicated that surface treatment ($P = .0001$) and instrument ($P = .0001$) influenced Ra measurements (Table 1). Measurement site as an assessment of spatial variability did not influence Ra values (diametrical: $P = .9859$; area: $P = .9824$). Measurement sequence, which assessed a user or repeated-measure influence, likewise had no effect on Ra determination ($P = .9990$). In the assessment of individual instrument accuracy, the interferometer was the most accurate in the prediction of SEM-based Ra ($P = .6688$) compared with the stylus ($P = .0839$). For a description of precision, the most precise instrument based on an aggregate CV for all measurements (Table 1) was the stylus ($CV =$

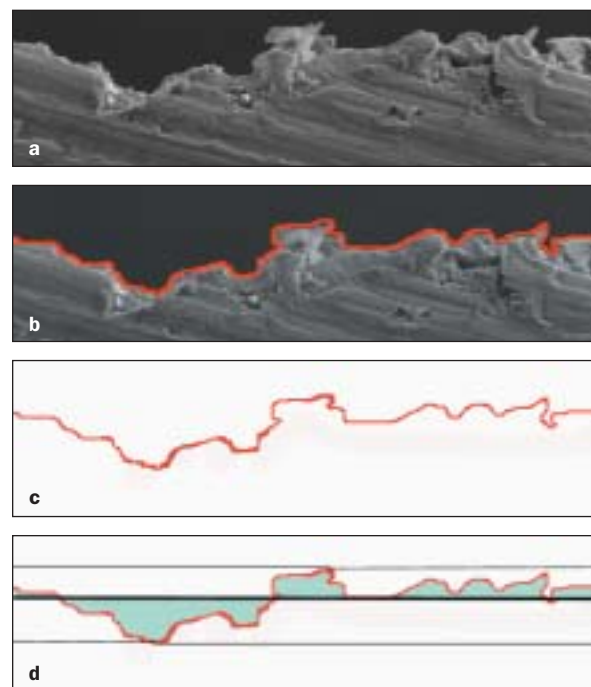


Fig 2 Illustrated protocol for direct determination of Ra from test sample disks. (a) An SEM image of a cross-sectional view of a TPS disk was made (original magnification $\times 400$). (b) A digital contour (red line) was drawn over the roughened surface profile. (c) The digital contour was isolated for roughness calculation. (d) Maximum and minimum horizontal lines were drawn from peak references, while the mean line was set by equating the curve areas (green shading) above and below it.

0.108), followed by the interferometer ($CV = 0.125$) and SEM ($CV = 0.273$).

DISCUSSION

The objective of this project was to characterize accuracy and precision associated with representative dental implant profilometry techniques. To satisfy this objective, mechanical and optical profilometers were used to quantify the roughness of 4 different surfaces and compare them with direct roughness calculations acquired from cross-sectional views analyzed using microscopy. Since implant surface quality has been shown to affect long-term stability, an industry-wide standardization of acceptable levels of accuracy and precision for each measurement device is necessary to facilitate consistent comparison of commercially available implants. The data collected in this study achieved the objective, providing a means for direct comparisons for the purpose of statistical assessment.

Roughness data collected from the literature indicate a broad range of roughness values for similar surface preparations using similar profilometers.

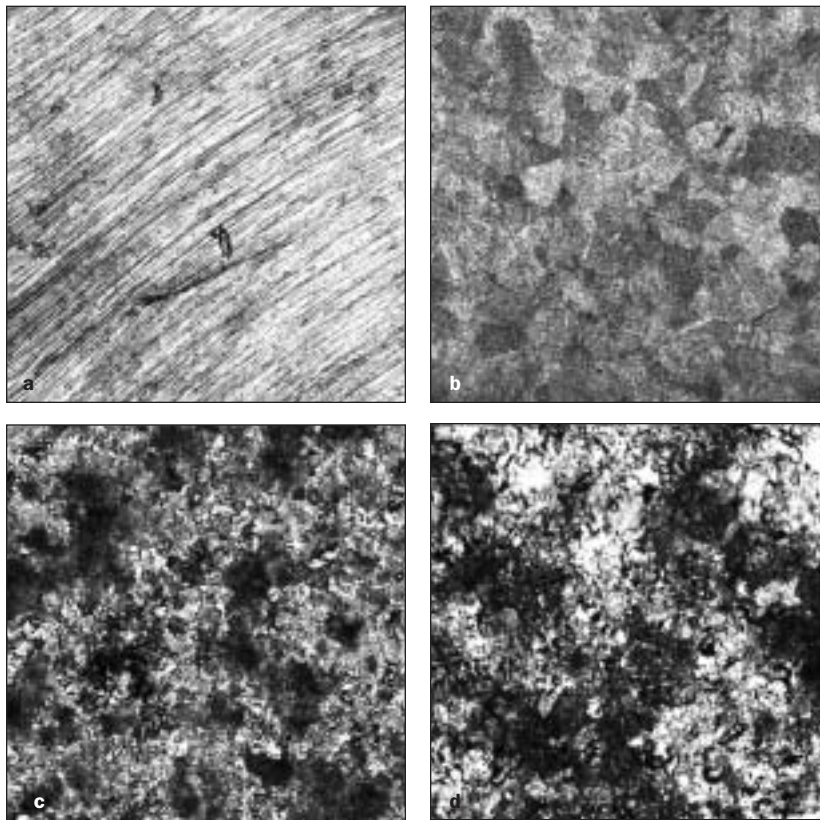


Fig 3 Representative LSCM images of (a) machined, (b) acid-etched, (c) HA-coated, and (d) TPS surfaces (original magnification $\times 320$).

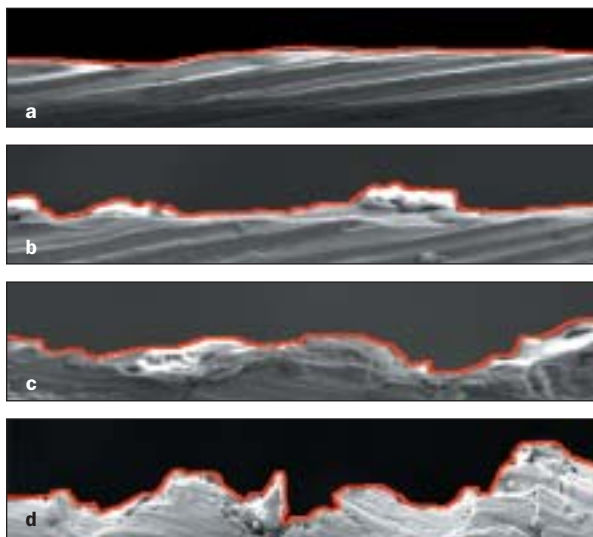


Fig 4 Representative cross-sectional SEM images of segments from (a) machined, (b) acid-etched, (c) HA-coated, and (d) TPS surfaces. The digital contour line (red) was used for direct calculation of Ra (original magnification $\times 400$).

Table 1 Ra Values in μm , Standard Errors (SE), and Coefficients of Variation (CV) for Each Surface Type

	Machined			Acid etched			HA coated			TPS		
	Mean	SE	CV	Mean	SE	CV	Mean	SE	CV	Mean	SE	CV
Stylus*	0.365	0.030	0.082	0.699	0.064	0.092	3.353	0.082	0.038	3.755	1.085	0.222
Interferometer [†]	0.327	0.002	0.054	0.727	0.014	0.144	5.368	0.126	0.073	6.088	0.834	0.228
SEM [‡]	1.200	0.184	0.306	2.486	0.286	0.230	4.260	0.795	0.373	5.911	0.539	0.183

*120 total measurements.

[†]240 total measurements.

[‡]16 total calculations were made using the Ra equation.

Stylus measurements in the present study were within a large range of Ra values (0.9 to 28.3 μm) found in Kitsugi and coworkers,¹⁶ Nakashima and associates,¹⁵ and Keller and colleagues.²⁶ Interferometer measurements were somewhat similar (0.29 to 10.8 μm) to those in Mehl and associates.²⁷ The difficulty of direct Ra comparisons, because of the contributions of uncontrolled influencing variables, highlights the need for standardization.

Although this work provides a unique basis of comparison using direct cross sections, there were limitations associated with this effort. These include the destructive nature of the process of sectioning the disks for SEM observation, optional filtering associated with interferometry, the potential destructiveness of the stylus tip, the difference between area measurements and linear measurements, variability in the normalized measurement length (L from the roughness equation), the relationship between disk geometry and dental implant geometry, and the direct mathematical calculation of Ra (SEM) versus the use of software algorithms (stylus and interferometer).

Future testing should overcome the limitations associated with quantifying instrument and sample variation. Measurements of different sites on threaded implants (peak, valley, and flank) would enable geometric influences to be isolated.²⁰ Comparisons between sample batches using measurements from the same instrument would provide a measure of the consistency in surface preparation. Additional surface treatments such as polishing, sandblasting, Al_2O_3 blasting, TiO_2 blasting, and CaP coating would provide an additional range of surface applications. The number of instruments should be expanded to include the atomic force microscope and LCSM. Measures of precision and accuracy could be investigated using traveling studies (ie, analysis of the same samples by multiple laboratories) as suggested by the American Society for Testing and Materials Committee on Medical and Surgical Materials and Devices.²⁸ Finally, examination of cell and tissue adhesion with dental implant surfaces²⁹ should ultimately quantify functional variability.

Area-scale analysis has been successful in demonstrating the influence of surface texture or roughness on adhesion.³⁰ The theory is based on a discrete bonding model, in which the macroscopic adhesive strength is derived from a finite number of discrete bonds at some finer scale. Each of the discrete bonds occupies some small but finite space on the substrate, and some small but finite force is required to rupture it. The discrete bonding model was found to be a reasonable explanation of the relation between roughness and adhesive strength

in a recent study using thermal spray coatings.³⁰ In this study, correlation coefficients approaching 0.9 were found for adhesive strength versus relative area at a sufficiently fine scale. The relative area is the normalized area of the rough surface at a particular scale. The area of a rough surface depends on the scale of observation³¹ where more surface area is observable at finer scales than at larger scales. Normalization is accomplished by dividing surface area by the nominal, or projected, area of the rough surface. The discrete bonding theory proposes that there is a scale that corresponds to the area required for each of the discrete bonds, and this is the scale of the relative area that will correlate best with the adhesive strength. This scale can be determined experimentally³⁰ and used phenomenologically to advance the understanding of the adhesive mechanisms and their interaction with surface textures. Future work will address this scale analysis relative to cellular adhesion with implant surfaces.

The overall results of this study indicate that the accuracy and precision of profilometers, eg, mechanical contact profilometers, scanning probe microscopes, and optical profilometers, may be strongly dependent upon the surface characterization technique. This variability may obscure the true nature of reported functional correlations between implant surface topography and osseointegration. Statistical standardization is strongly advocated to strengthen reported relationships.

ACKNOWLEDGMENTS

The authors recognize the valuable technical contributions of Mr Torbjorn S. Bergstrom, the WPI Surface Metrology Laboratory; Dr Ronald R. Biederman, the WPI Microscopy Facility; Mr Eric Felkel and Mr Stephen R. Kobak, the Zygo Corporation; and Dr Douglas J. Taatjes, the University of Vermont Cell Imaging Facility. Dr Allen H. Hoffman and Dr Mark W. Richman contributed constructive comments. Partial funding for this project was provided by Implant Innovations and the Office for Academic Affairs, Worcester Polytechnic Institute.

REFERENCES

1. Bränemark P-I, Hansson BO, Adell R, et al. Osseointegrated implants in the treatment of the edentulous jaw. Experience from a 10-year period. *Scand J Plast Reconstr Surg* 1977;11 (suppl 16):1-132.
2. Boyan BD, Hummert TW, Dean DD, Schwartz Z. Role of material surfaces in regulating bone and cartilage cell response. *Biomaterials* 1996;17:137-146.
3. Caulier H, Vercaigne S, Naert I, et al. The effect of Ca-P plasma-sprayed coatings on the initial bone healing of oral implants: An experimental study in the goat. *J Biomed Mater Res* 1997;34:121-128.

4. Chehroudi B, McDonnell D, Brunnette DM. The effects of micromachined surfaces on formation of bonelike tissue on subcutaneous implants as assessed by radiography and computer image processing. *J Biomed Mater Res* 1997;34: 279–290.
5. Cochran DL, Schenk RK, Lussi A, Higginbottom FL, Buser D. Bone response to unloaded and loaded titanium implants with a sandblasted and acid-etched surface: A histometric study in the canine mandible. *J Biomed Mater Res* 1998; 40:1–11.
6. Gotfredsen K, Wennerberg A, Johansson C, Skovgaard LT, Hjørting-Hansen E. Anchorage of TiO₂-blasted, HA-coated, and machined implants: An experimental study with rabbits. *J Biomed Mater Res* 1995;29:1223–1231.
7. Martin JY, Schwartz Z, Hummert TW, et al. Effect of titanium surface roughness on proliferation, differentiation, and protein synthesis of human osteoblast-like cells (MG63). *J Biomed Mater Res* 1995;29:389–401.
8. Wennerberg A, Albrektsson T, Johansson C, Andersson B. Experimental study of turned and grit-blasted screw-shaped implants with special emphasis on effects of blasting material and surface topography. *Biomaterials* 1996;17:15–22.
9. Wennerberg A. Importance of surface roughness for implant incorporation. *Int J Machine Tools Manufacture* 1998;38: 657–662.
10. Piattelli A, Trisi P. Bone ingrowth into hydroxyapatite coating: A light microscopy and laser scanning microscopy study. *Biomaterials* 1993;14:973–977.
11. Buser D, Schenk RK, Steinemann S, et al. Influence of surface characteristics on bone integration of titanium implants. A histomorphometric study in miniature pigs. *J Biomed Mater Res* 1991;25:889–902.
12. Hansson S. Surface roughness parameters as predictors of anchorage strength in bone: A critical analysis. *J Biomech* 2000;33:1297–1303.
13. Ogiso M, Nakabayashi N, Matsumoto T, Yamamura M, Lee RR. Adhesive improvement of the mechanical properties of a dense HA-cemented Ti dental implant. *J Biomed Mater Res* 1996;30:109–116.
14. Bhushan B, Gupta BK. *Handbook of Tribology*. New York: McGraw-Hill, 1991:7.1–7.25.
15. Nakashima Y, Hayashi K, Inadome T, et al. Hydroxyapatite-coating on titanium arc sprayed titanium implants. *J Biomed Mater Res* 1997;35:287–298.
16. Kitsugi T, Nakamura T, Oka M, et al. Bone bonding behavior of titanium and its alloys when coated with titanium oxide and titanium silicate. *J Biomed Mat Res* 1996;32:149–156.
17. Whitehouse DJ. *Handbook of Surface Metrology*. Philadelphia: Institute of Physics Publishing, 1994:409–421.
18. Bennett JM, Mattsson L. *Introduction to Surface Roughness and Scattering*. Washington, DC: Optical Society of America, 1989:7–12.
19. Clark MB. *Standardization of Profilometry Measurements in Dental Implants* [thesis]. Worcester, MA: Worcester Polytechnic Institute, 2000.
20. Wennerberg A, Albrektsson T. Suggested guidelines for the topographic evaluation of implant surfaces. *Int J Oral Maxillofac Implants* 2000;15:331–344.
21. Thomas TR. *Rough Surfaces*, ed 2. London: Imperial College Press, 1999:1–278.
22. Bourauel C, Fries T, Drescher D, Plietsch R. Surface roughness of orthodontic wires via atomic force microscopy, laser specular reflectance, and profilometry. *Eur J Orthod* 1998; 20:79–92.
23. Al-Nawas B, Grotz KA, Gotz H, et al. Validation of three-dimensional surface characterising methods: Scanning electron microscopy and confocal laser scanning microscopy. *Scanning* 2001;23:227–231.
24. Brown CA, Johnsen WA, Hult KM. Scale-sensitivity, fractal analysis and simulations. *Int J Machine Tools Manufacture* 1998;18:633–637.
25. Vernino AR, Kohles SS, Holt RA, Lee HM, Caudill RF, Kenealy JN. Dual-etched implants loaded after 1- and 2-month healing periods: A histologic comparison in baboons. *Int J Periodontics Restorative Dent* 2002;22:399–407.
26. Keller JC, Stanford CM, Wightman JP, Draughn RA, Zaharias R. Characterization of titanium implant surfaces. *J Biomed Mater Res* 1994;28:939–946.
27. Mehl A, Gloger W, Kunzelmann K-H, Hickel R. A new optical 3-D device for the detection of wear. *J Dent Res* 1997;76:1799–1807.
28. American Society for Testing and Materials, ASTM Committee F04 on Medical and Surgical Materials and Devices. *Annual Book of ASTM Standards*, vol 13.01. Philadelphia: Author, 2000.
29. Gianoli DJ, Kohles SS, Burnham NA, Clark MB, Brown CA, Kenealy JN. The feasibility of atomic force microscopy as a cytodetachment technique to quantify osteoblastic adhesion with implant surfaces. In: Enderle JD, Macfarlane LL (eds). *Proceedings of the Institute of Electrical and Electronics Engineers 27th Annual Northeast Bioengineering Conference*, March 30–April 1, 2001, Storrs, CT:5–6.
30. Brown CA, Siegmans S. Fundamental scales of adhesion and area-scale fractal analysis. *Int J Machine Tools Manufacture* 2001;41:1927–1933.
31. Brown CA, Charles PD, Johnsen WA, Chesters S. Fractal analysis of topographic data by the patchwork method. *Wear* 1993;161:61–67.